VER
Vascular & Endovascular Review

Computational Discovery of Potential Acyl-CoA: Cholesterol Acyltransferase Inhibitors Using Structure-Based Virtual Screening

Shainda Laeeq*[1], Vishal Dubey[2]

*[1]Assistant Professor, Faculty of Pharmacy, Maharana Pratap College of Pharmacy, Kothi Mandhana, Kanpur- 209217
[2]Professor, Faculty of Pharmacy, Naraina Vidyapeeth Group of Institutions, Panki Gangaganj, Kanpur- 208020

* Corresponding Author
Email: shaindalaeeq786@gmail.com

ABSTRACT

Hyperlipidemia is a major metabolic disorder characterized by elevated levels of plasma lipids, including cholesterol and triglycerides, which contribute significantly to the development of atherosclerosis and subsequent cardiovascular complications such as angina pectoris, myocardial infarction, and cardiac arrest. Acyl-CoA:cholesterol acyltransferase (ACAT) is a key enzyme involved in intracellular cholesterol esterification, and its inhibition represents a promising therapeutic strategy for the management of hyperlipidemia. In the present study, molecular modeling approaches were employed to identify novel ACAT inhibitors with potential antihyperlipidemic activity. Pharmacophore models were developed based on structurally diverse, known ACAT inhibitors to elucidate essential molecular features governing enzyme inhibition. Following an extensive literature survey, a focused virtual library of heterocyclic compounds was designed to explore alternative lipid-lowering targets and to determine whether the observed hypolipidemic effects could be attributed to ACAT inhibition. Heterocyclic scaffolds, comprising ring systems containing atoms of at least two distinct elements, are known to play a pivotal role in drug discovery due to their versatile biological activities. Representative heterocycles such as quinoline, benzothiophene, indole, benzofuran, benzothiazole, benzimidazole, and benzoxazole were considered as structural templates for pharmacophore development. Among these, benzoxazole and benzothiazole moieties were selected as key pharmacophoric cores for the design of novel derivatives. These compounds were subjected to in silico screening using molecular docking and related computational techniques to assess their interaction with the ACAT active site.Several designed derivatives demonstrated favorable docking scores and strong binding affinities toward the ACAT receptor, indicating potential inhibitory activity. These promising heterocyclic compounds will be further evaluated through advanced computational studies and experimental assays to identify lead candidates for the development of novel antihyperlipidemic agents targeting ACAT.

KEYWORDS: Hyperlipidemia, Obesity, Open Babel, Docking studies, Binding affinity..

How to Cite: Shainda Laeeq, Vishal Dubey, (2025) Computational Discovery of Potential Acyl-CoA: Cholesterol Acyltransferase Inhibitors Using Structure-Based Virtual Screening, Vascular and Endovascular Review, Vol.8, No.8s, 196-203.

INTRODUCTION

Hyperlipidemia, characterized by abnormally elevated levels of plasma cholesterol, represents a major risk factor for atherosclerosis, visceral obesity, and associated cardiovascular disorders [1]. Reduction of cholesterol levels can be achieved through the inhibition of cholesterol biosynthesis or absorption within cells [2]. Currently, inhibitors of human 3-hydroxy-3-methylglutaryl coenzyme A reductase (hHMGR), commonly known as statins, constitute the most effective class of cholesterol-lowering agents. However, the clinical use of statins is often limited by adverse effects, including myotoxicity, hepatotoxicity, and, in severe cases, rhabdomyolysis [3]. These side effects primarily arise from the inhibition of HMG-CoA reductase, which interferes with the synthesis of nonsteroidal isoprenoid molecules essential for diverse cellular functions [4]. Compared to HMG-CoA reductase, acyl-CoA:cholesterol acyltransferase (ACAT), a key enzyme in the downstream cholesterol biosynthetic pathway, has emerged as an attractive alternative therapeutic target for the treatment of hyperlipidemia [5]. ACAT catalyzes the esterification of cholesterol, representing a critical step in cholesterol metabolism. Inhibition of ACAT can effectively prevent intracellular cholesterol deposition without disrupting isoprenoid biosynthesis [6]. Owing to this unique mechanistic advantage, ACAT inhibitors hold significant promise as next-generation antihyperlipidemic agents.To date, both chemical synthesis [7] and genetic engineering approaches [8] have been employed for the discovery of novel ACAT inhibitors; however, these methods are often time-consuming and cost-intensive. Alternatively, Traditional Chinese Medicine (TCM) has demonstrated considerable efficacy in managing hyperlipidemia, offering low cost and minimal adverse effects [9,10]. This underscores the importance of identifying new, potent ACAT inhibitors through efficient and cost-effective strategies. In a recent study, molecular docking and virtual screening techniques were utilized to identify potential ACAT inhibitors [11]; however, the absence of experimental validation limited the reliability of the computational findings. Therefore, integrating *in silico* modeling with subsequent biological assays remains crucial for the accurate identification and validation of promising ACAT inhibitors as novel antihyperlipidemic agents.In the present study, a systematic *in silico* approach was employed to identify potential acyl-CoA:cholesterol acyltransferase (ACAT) inhibitors using molecular modeling techniques. Initially, several pharmacophore models were generated based on the structural and functional features of known ACAT inhibitors. The optimal pharmacophore model was selected and utilized for virtual screening to identify potential ACAT inhibitors using AutoDock 4.3. Molecular docking studies were subsequently performed to refine the hits obtained from pharmacophore screening and to analyze the protein–ligand binding interactions within the ACAT active site. Furthermore, molecular dynamics (MD) simulations were

conducted to evaluate the conformational stability and dynamic behavior of the protein–ligand complexes. Candidate compounds were prioritized based on their pharmacophore fit values, docking scores, and key interactions with essential amino acid residues in the ACAT binding pocket. Overall, this study provides a robust computational framework for the discovery of novel ACAT inhibitors and identifies promising candidate molecules for the potential treatment of hyperlipidemia. Heterocyclic compounds constitute a vital class of organic molecules characterized by ring structures containing at least two different elements, typically carbon along with heteroatoms such as nitrogen, oxygen, or sulfur. In contrast to homocyclic compounds, which contain rings composed solely of carbon atoms, heterocyclic compounds exhibit diverse electronic and chemical properties arising from the incorporation of heteroatoms into their ring systems. Although some heterocycles are inorganic, the majority of biologically active heterocyclic compounds are organic in nature and play crucial roles in medicinal chemistry due to their structural versatility and pharmacological relevance. Heterocyclic compounds can be broadly classified based on their electronic configuration into saturated and unsaturated systems. Saturated heterocycles, such as tetrahydrofuran and piperidine, display chemical behavior similar to their acyclic analogs (ethers and amines, respectively), while unsaturated heterocycles form the core structures of numerous bioactive compounds. Five- and six-membered unsaturated heterocycles, including furan, thiophene, pyrrole, and pyridine, are of particular interest due to their aromatic stability and diverse reactivity. Fused heterocyclic systems represent another important subclass wherein heterocycles are conjugated with benzene or other aromatic rings, resulting in enhanced stability and biological activity. Notable examples include quinoline (pyridine fused with benzene), benzothiophene (thiophene fused with benzene), indole (pyrrole fused with benzene), benzofuran (furan fused with benzene), benzothiazole, benzimidazole, and benzoxazole. Larger fused systems, such as acridine, dibenzothiophene, carbazole, and dibenzofuran, arise from the fusion of two benzene rings with heterocyclic cores.The reactivity of heterocycles is strongly influenced by the participation of heteroatoms in the π-electron system and by ring strain. Three-membered heterocycles, due to their angular strain, tend to be more reactive, whereas five- and six-membered heterocycles exhibit greater thermodynamic stability. Common three-membered systems containing a single heteroatom include aziridine, oxirane, and thiirane, which serve as important intermediates in organic synthesis. The unique electronic properties, stability, and structural adaptability of heterocycles make them indispensable scaffolds in the rational design of new pharmacologically active agents, including potential ACAT inhibitors for antihyperlipidemic therapy.Heterocyclic frameworks represent a fundamental structural motif in the majority of marketed pharmaceuticals. Notably, among the top five U.S. small-molecule drugs by retail sales in 2019, four compounds either consist entirely of or incorporate heterocyclic fragments within their molecular structures (Figure 1). Collectively, these four heterocycle-containing drugs accounted for approximately USD 27.4 million in sales, representing nearly 80% of the total revenue generated by the top five prescription medications.

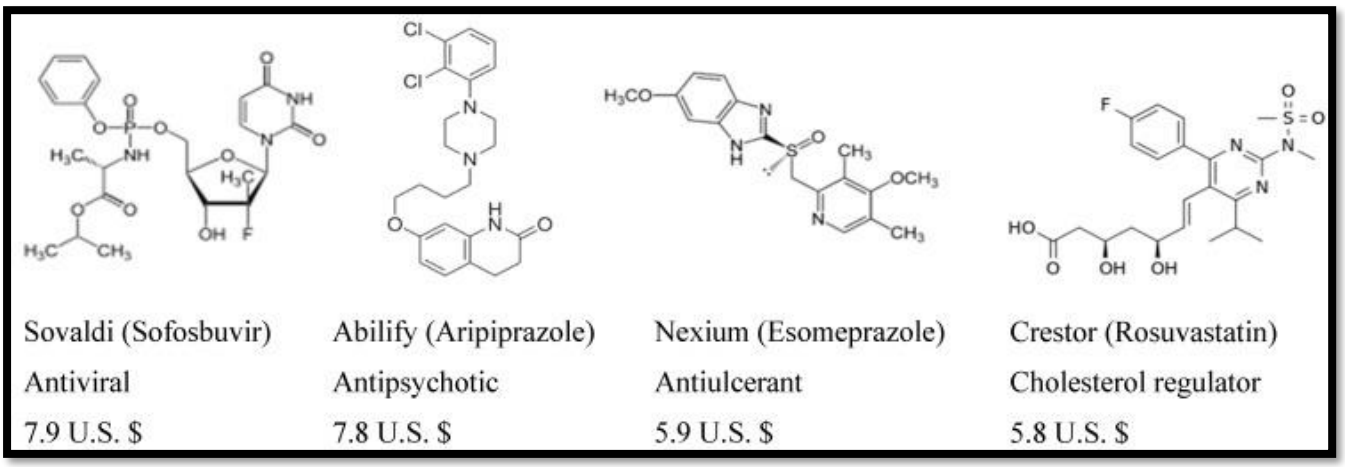

Fig. 1: Top five U.S. prescription drugs (2019) containing heterocyclic moieties and their retail sales

The design and development of modern pharmaceuticals are deeply rooted in the strategic incorporation of heterocyclic fragments that impart specific physicochemical and pharmacokinetic properties to drug molecules. The inclusion of such heterocyclic moieties enables fine-tuning of biological potency and selectivity through bioisosteric modifications, as well as optimization of key parameters such as lipophilicity, polarity, and aqueous solubility. These structural modifications can significantly influence the mechanism of action and overall pharmacodynamic profile of the resulting therapeutic agents, facilitating the development of molecularly targeted drugs. However, despite their structural versatility and pharmacological potential, the translation of heterocyclic compounds into clinically approved drugs continues to face challenges related to synthetic complexity, pharmacokinetic limitations, and toxicity concerns.Among various heterocyclic frameworks, benzothiazole and benzoxazole represent particularly important structural motifs found in numerous natural products and pharmacologically active compounds [1]. These bicyclic systems are recognized as privileged scaffolds in medicinal chemistry, owing to their ability to engage in diverse molecular interactions with biological targets. The benzothiazole and benzoxazole rings serve as core pharmacophores in the design of a wide range of therapeutically relevant agents, exhibiting activities such as antiulcer [2], antioxidant [3], HIV reverse transcriptase inhibitory [4], anticancer [5], antihelmintic [6], antimicrobial [7], and antihistaminic [8] properties. Their broad pharmacological profile and favorable drug-like characteristics make them promising candidates for the development of novel bioactive molecules in contemporary drug discovery.

MOLECULAR MODELING METHOD:

Identification of target and its validation: Target ACAT was identified and protein PDB id: 1WL5 was selected and downloaded from protein data base website http://www.rcsb.org/ db/explore/ explore.do? structureId=1WL5).

Scaffold Selection: After doing literature review we found that benzthiazole and benzoxazole moiety can be undergone for CADD studies against ACAT enzyme for antihyperlipidemic agents.

Designing Lead library: Pharmacophore was designed as lead first and then its derivatives using ChemDraw Ultra 12.0 were designed. The library was based on Lipinski's rule of five. Care was taken not to include heavy atoms or carcinogenic atoms to the molecule.

Screening the Virtual library: In order to select a lower number of compounds for screening for bioactivity against the specific drug target, VS is commonly described as a sequence of filter techniques. Only when the target structure is available, VS is frequently followed by ligand- and/or structure-based techniques after a quick evaluation of a compound's druglikeness [12]. Three groups of increasingly complicated and computationally demanding computational techniques are used in VS. In actual use, they are frequently combined. These include evaluations based on target-specific pharmacophores, which are condensed representations of the salient characteristics of the target system or ligand [13], evaluations based on these two (2D) property profiles of properties, detailed 3D structure modelling of receptor-ligand interaction, and evaluations based on target-specific pharmacophores [14].

To uncover new scaffolds, ligand-based virtual screening was conducted for the lead library that binds to the ACAT receptor (1WL5). This was followed by a binding-score function evaluation of the docked conformation.

Preparation of 3D ligand: - It was created a modest library of ligands. Through the use of the Open BabelGUI programme (software used to read, write, and convert over 110 chemical file formats), ligand structure drawn was stored in.mol format was transformed to .pdbqt format. The MGLTools programme loaded this PDB file in 3D format and automatically determined the number of rotatable bonds, calculated atom charges, and combined polar hydrogen. Now save the ligand as a.pdbqt file.

Preparation of protein: - A protein with the PDB identifier 1WL5 was downloaded. View the Protein in AutoDock Tools by opening it. It was first prepared by removing the ligand and water, and then hydrogen was added to the protein structure. Only the protein that was free of bound ligand and water was saved as a PDB file (protein). Then add polarity and Kollman charges. The file was currently saved in PDBQT format.

Receptor and Ligand Preparation: Now we chose macromolecule 1WL5.pdbqt. Then input the ligand and select the amino acids in the target receptor. Go to the Grid selection and select Grid box. It was set on the region of binding pocket (grid dimensions are as follows)

center_x = 60.1232254999; center_y =55.4152206065; center_z = 72.3980596464;
size_x = 25.0; size_y = 25.0; size_z = 25.0

Now we closed it by saving the current. The output was saved in .gpf format. After running the Autogrid for docking the receptor protein and ligands, Selection of parameter was done in genetic Algorithm and output calculated via Lamarkian was saved in .dpf format.

Molecular Receptor-Ligand Docking: We ran the AutoDock for the minimized receptor and ligands. To ascertain the potential of the molecules docked, the receptor-ligand complex is investigated.

Analyze: Conformation of macromolecule (protein) was analyzed and visualized with ligand through Discovery studio Visualizer.

TABLE 1. COMPOUND WITH BINDING ENERGY AND RMS VALUE

Compound	Binding Energy	Kl (Nm)	Intermolecular Energy	Internal Energy	Torsional Energy	Unbound Extended Energy	Cluster Rms	Ref Rms
C1	-8.35	751.71	-10.14	-0.6	1.79	-0.6	0	48.23
C2	-7.79	1.96uM	-9.87	-0.54	2.09	-0.54	0	46.25
C3	-9.79	66.28nM	-11.88	-0.78	2.09	-0.78	0	49.37
C4	-7.64	2.51uM	-10.03	-0.81	2.39	-0.81	0	47.01
C5	-7.71	2.22uM	-9.5	-0.65	1.79	-0.65	0	48
C6	-8.21	965.3nM	-10.29	-0.76	2.09	-0.76	0	50.82
C7	-8.4	691.45nM	-10.49	-0.59	2.09	-0.59	0	46.87
C8	-8.31	815.42nM	-10.39	-0.76	2.09	-0.76	0	47.5
C9	-9.66	82.5nM	-11.15	-0.97	1.49	-0.97	0	48.99

C10	-9.88	57.74nM	-11.55	-1.06	1.79	-1.06	0	45.55
C11	-8.66	79.87nM	-11.47	-0.96	1.79	-0.96	0	46.39
C12	-8.6	493.66nM	-10.39	-0.88	1.79	-0.88	0	47.13
C1S	-8.5	589.94nM	-10.29	-0.74	1.79	-0.74	0	48.81
C2S	-5.65	72.39uM	-7.74	-0.63	2.09	-0.63	0	54.06
C3S	-5.97	41.93uM	-8.06	-0.23	2.09	-0.23	0	49.62
C4S	-6.97	7.78uM	-9.36	-0.91	2.39	-0.91	0	68.02
C5S	-8.54	545.44nM	-10.63	-0.92	2.09	-0.92	0	48.15
C6S	-8.36	741.7nM	-10.45	-0.95	2.09	-0.95	0	48.06
C7S	-8.96	268.55nM	-11.05	-1.12	2.09	-1.12	0	47.82
C8S	-9.37	134.62nM	-11.76	-0.95	2.39	-0.95	0	48.37

STRUCTURES FOR VIRTUAL SCREENING

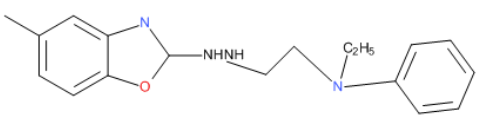

C10(-9.88)

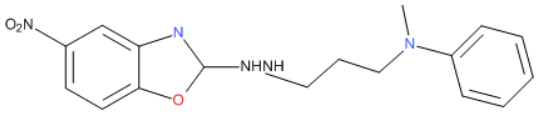

C3(-9.79)

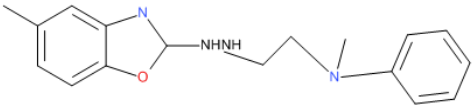

C9(-9.66)

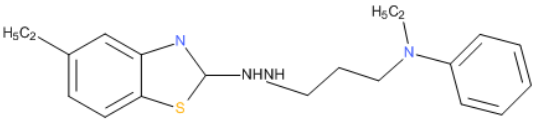

C8S(-9.37)

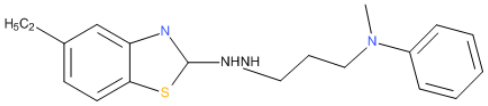

C7S(-8.96)

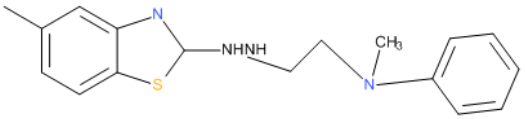

C11S(-8.66)

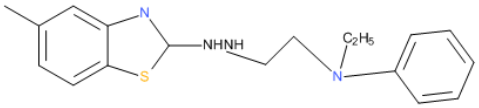

C12(-8.6)

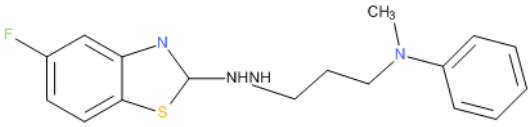

C5S(-8.54)

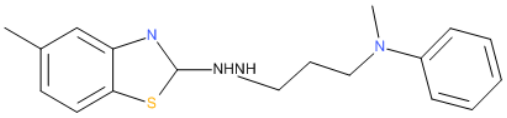

C1S(-8.5)

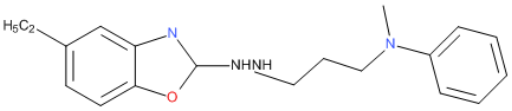

C7(-8.4)

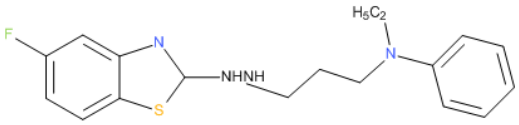

C6S(-8.36)

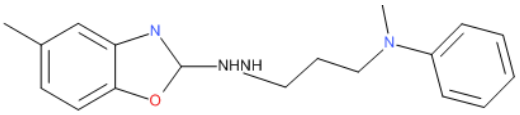

C1(-8.35)

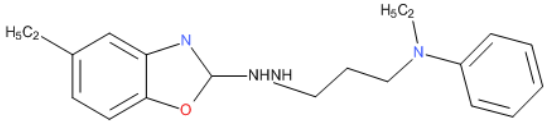

C8(-8.31)

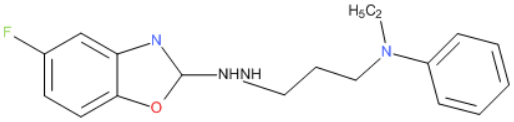

C6(-8.21)

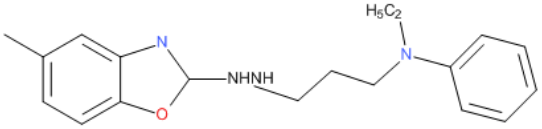

C2(-7.79)

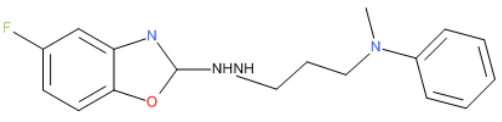

C5(-7.71)

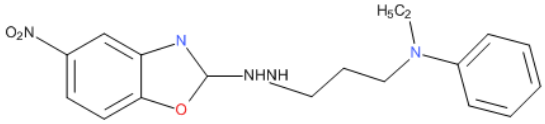

C4(-7.64)

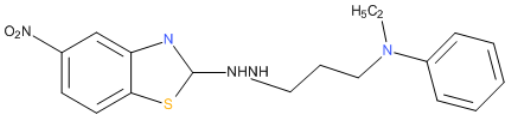

C4S(-6.97)

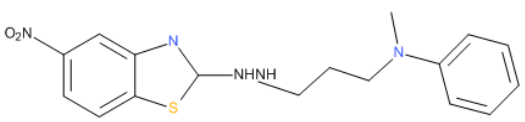

C3S(-5.97)

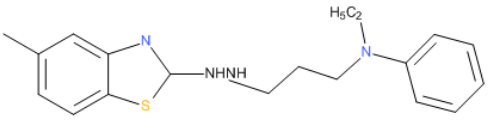

C2S(-5.65)

BEST FIVE DOCKED COMPOUND SHOWING THE AMINO ACID BINDING IN TARGET RECEPTOR

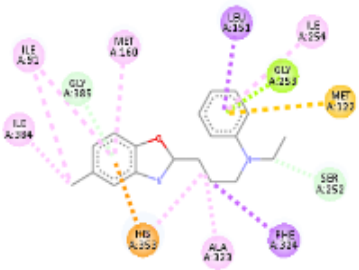

C10

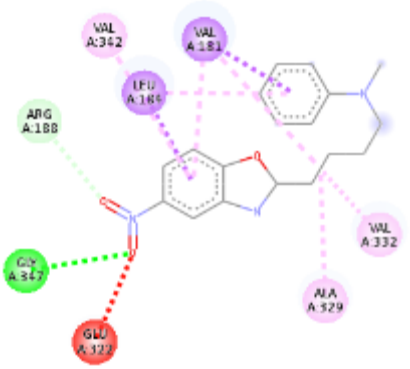

C3

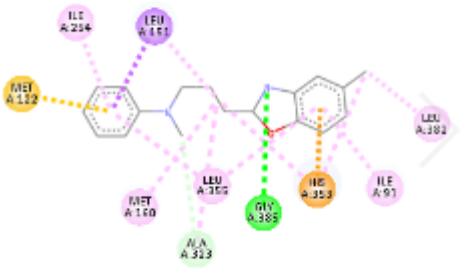

C9

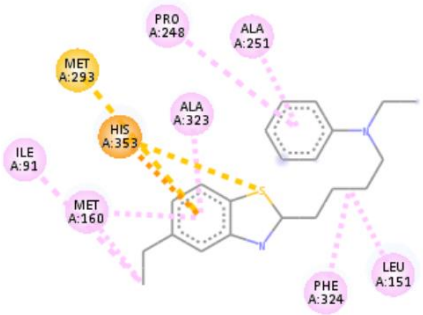

C8S

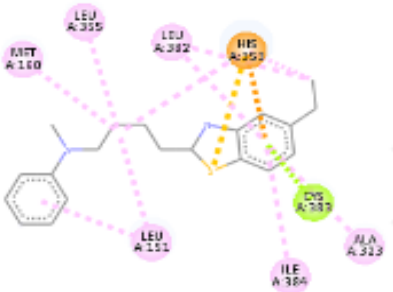

C7S

RESULT

Molecular docking studies were performed using **AutoDock 4.3** to evaluate the binding affinities and interaction profiles of the designed compounds against the **acyl-CoA:cholesterol acyltransferase (ACAT)** enzyme. The docking simulations revealed that the selected ligands exhibited favorable binding energies and strong affinity toward the ACAT active site. Docking scores and root-mean-square deviation (RMSD) values were recorded to assess the reliability and stability of the predicted binding conformations.

Based on prior literature, the key amino acid residues identified as part of the ACAT active site included **Tyr89, Leu169, Phe252, Ala262, Met316, Ala321, Leu348, His353, Ile378, Cys380, Gly383, Ala400, Phe456,** and **Leu460**. Analysis of the two-dimensional and three-dimensional interaction diagrams for the top five docked compounds—**C10, C3, C9, C8S, and C7S**—showed high docking scores of **−9.88, −9.79, −9.66, −9.37,** and **−8.96 kcal/mol**, respectively.

Among these, compounds **C10, C3,** and **C9** demonstrated the most favorable binding poses within the ACAT active site. These ligands exhibited multiple **hydrogen bonding interactions** with residues **Gly385, Gly359, Ser94,** and **Ala323**, contributing to enhanced binding stability. Additionally, **cation–π interactions** were observed between the imidazole ring of **His353** and the aromatic systems of **C10, C3, C9, C8S,** and **C7S**. Compounds **C8S** and **C7S** also displayed **sulfur interactions** with **Met160**, further stabilizing the complex.

Moreover, **aromatic and hydrophobic interactions** were detected between the ligands and residues **Gly385, Ile384, Ile91, Ala323, Leu355,** and **Leu382**, while **C7S** exhibited an additional **lone pair–π interaction** with **Cys383**. The terminal alkyl chains of these compounds showed significant **hydrophobic contacts** with **Ala323, Met160, Phe324,** and **Leu355**, reinforcing the overall binding affinity.

The docking results suggest that compounds **C10, C3,** and **C9** exhibit optimal geometric fit and strong non-covalent interactions within the ACAT binding pocket. These findings indicate that the identified heterocyclic derivatives may serve as promising lead candidates for the development of potent **ACAT inhibitors** with potential antihyperlipidemic activity.

TABLE 2. AMINO ACID INTERACTION WITH THE COPMUNDS

COMPOUNDS	LEU	VAL	HIS	ILE	GLY	MET	ARG	GLU	ALA	PRO	CYS	PHE	LYS	SER	ASN	THR	TYR
C10	151		353	91 254 384	253 385	122 160			323			324					
C3	382 184 151 355	392	353 159	91 254 384	93 95 253 347 359 356 385	160 293	188	322	251 329		283	238 324	181	94 252 358	321		
C9	355 382 151		353	91 254	253	122 160			323								
C8S	151		353	91		160 293			251 323	248		324					
C7S	82 151 382 355		353	384		160			323		384						

2D AND 3D TARGET RECEPTOR AND LIGAND INTERACTIONS

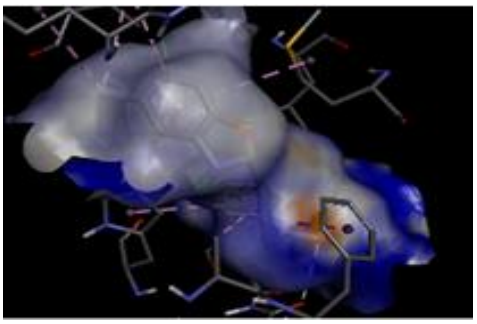

C10

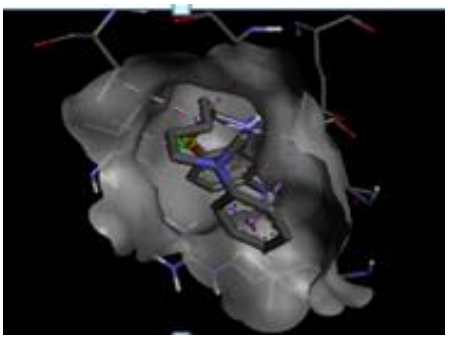

C3

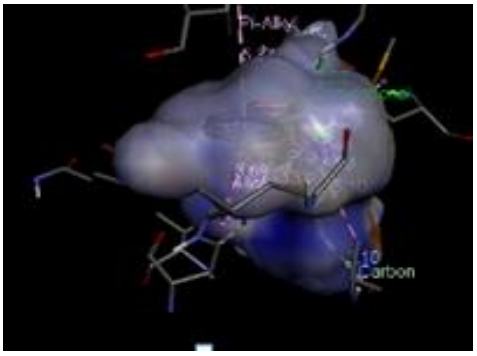

C9

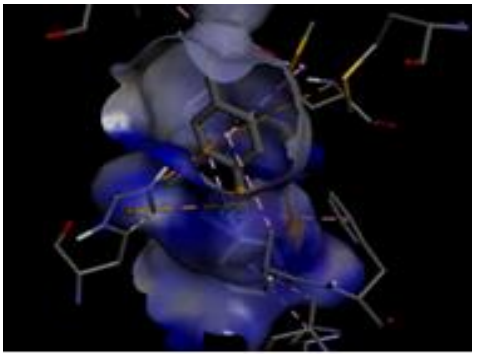

C8S

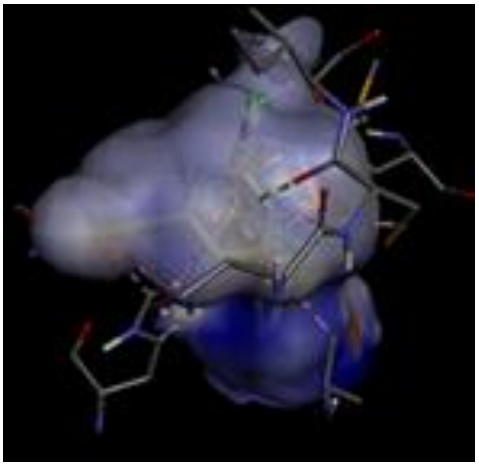

C7S

CONCLUSION

The compounds **C10, C3, C9, C8S,** and **C7S** emerged as promising candidates for the development of novel antihyperlipidemic agents with potentially favorable safety profiles. The molecular docking analysis demonstrated a strong and well-defined fit of these ligands within the active site of the **acyl-CoA:cholesterol acyltransferase (ACAT)** enzyme. Significant **alkyl interactions** were observed with key residues **Met160, Phe324, Ala323,** and **Leu355**, while **aromatic interactions** were noted with **His353, Gly385, Ile91, Leu355,** and **Ala323**, contributing to enhanced binding affinity and complex stability.These findings indicate that the identified heterocyclic derivatives possess structural features conducive to effective ACAT inhibition. Future work will focus on the **chemical synthesis and pharmacological evaluation** of these lead compounds to validate their inhibitory potential and to establish their efficacy as **novel antihyperlipidemic agents**.

Conflict of Interest:

There is no conflict of interest between authors.

REFERENCES

1. Ewes W. A.; Elmorsy M. A.; El-Messery S. M.; Nasr M. N. A. Synthesis, biological evaluation and molecular modeling study of [1,2,4]-Triazolo[4,3-*c*] quinazolines: New class of EGFR-TK inhibitors. *Bioorg. Med. Chem.* 2020, 28, 115373. 10.1016/j.bmc.2020.115373.
2. Shafei A.; El-Bakly W.; Sobhy A.; Wagdy O.; Reda A.; Aboelenin O.; Marzouk A.; El Habak K.; Mostafa R.; Ali M. A.; Ellithy M. A review on the efficacy and toxicity of different doxorubicin nanoparticles for targeted therapy in metastatic breast cancer. *Biomed. Pharmacother.* 2017, 95, 1209–1218. 10.1016/j.biopha.2017.09.059.
3. Hassan G. S.; Georgey H. H.; Mohammed E. Z.; George R. F.; Mahmoud W. R.; Omar F. A. Mechanistic selectivity investigation and 2D-QSAR study of some new antiproliferative pyrazoles and pyrazolopyridines as potential CDK2 inhibitors. *Eur. J. Med. Chem.* 2021, 218, 113389. 10.1016/j.ejmech.2021.113389.
4. Lemmon M. A.; Schlessinger J. Cell signaling by receptor tyrosine kinases. *Cell* 2010, 141, 1117–1134. 10.1016/j.cell.2010.06.011.
5. Kim M.; Baek M.; Kim D. J. Protein Tyrosine signaling and its potential therapeutic implications in carcinogenesis. *Curr. Pharm. Des.* 2017, 23, 4226–4246. 10.2174/1381612823666170616082125
6. Bansal R.; Malhotra A. Therapeutic progression of quinazolines as targeted chemotherapeutic agents. *Eur. J. Med. Chem.* 2021, 211, 113016. 10.1016/j.ejmech.2020.113016.
7. Mokhtar A. M.; El-Messery S. M.; Ghaly M. A.; Hassan G. S. Targeting EGFR tyrosine kinase: Synthesis, *in vitro* antitumor evaluation, and molecular modeling studies of benzothiazole-based derivatives. *Bioorg. Chem.* 2020, 104, 104259. 10.1016/j.bioorg.2020.104259.
8. Zhang H.; Berezov A.; Wang Q.; Zhang G.; Drebin J.; Murali R.; Greene M. I. ErbB receptors: from oncogenes to targeted cancer therapies. *J. Clin. Invest.* 2007, 117, 2051–2058. 10.1172/JCI32278.
9. Othman I. M. M.; Alamshany Z. M.; Tashkandi N. Y.; Gad-Elkareem M. A. M.; Anwar M. M.; Nossier E. S. New pyrimidine and pyrazole-based compounds as potential EGFR inhibitors: synthesis, anticancer, antimicrobial evaluation and computational studies. *Bioorg. Chem.* 2021, 114, 105078. 10.1016/j.bioorg.2021.105078.
10. Ahmed M. F.; Santali E. Y.; El-Deen E. M. M.; Naguib I. A.; El-Haggar R. Development of Pyridazine Derivatives as Potential EGFR inhibitors and Apoptosis Inducers: Design, Synthesis, Anticancer Evaluation, and Molecular Modeling Studies. *Bioorg. Chem.* 2021, 106, 104473. 10.1016/j.bioorg.2020.104473.
11. Capdevila J.; Elez E.; Macarulla T.; Ramos F. J.; Ruiz-Echarri M.; Tabernero J. Anti-epidermal growth factor receptor monoclonal antibodies in cancer treatment. *Cancer Treat. Rev.* 2009, 35, 354–363. 10.1016/j.ctrv.2009.02.001.
12. Muegge I (2008) Synergies of virtual screening approaches. Mini Rev Med Chem 8: 927-933.
13. Zheng W, Cho SJ, Tropsha A (1998) Rational combinatorial library design. 1. Focus-2D: a new approach to the design of targeted combinatorial chemical libraries. J Chem Inf Comput Sci 38: 251-258.

14. Van Drie JH, Weininger D, Martin YC (1989) ALADDIN: an integrated tool for computer-assisted molecular design and pharmacophore recognition from geometric, steric, and substructure searching of three-dimensional molecular structures. J Comput Aided Mol Des 3: 225-251.